Monthly Notices
of the
ROYAL ASTRONOMICAL SOCIETY

MNRAS **456,** L40–L44 (2016) doi:10.1093/mnrasl/slv173

CO luminosity function from *Herschel*-selected galaxies and the contribution of AGN

L. Vallini,[1,2]★ C. Gruppioni,[2] F. Pozzi,[1,2] C. Vignali[1,2] and G. Zamorani[2]

[1]*Dipartimento di Fisica e Astronomia, Universitá di Bologna, viale Berti Pichat 6/2, I-40127 Bologna, Italy*
[2]*INAF - Osservatorio Astronomico di Bologna, via Ranzani 2, I-40127 Bologna, Italy*

Accepted 2015 October 29. Received 2015 October 29; in original form 2015 July 3

ABSTRACT

We derive the carbon monoxide (CO) luminosity function (LF) for different rotational transitions [i.e. (1–0), (3–2), (5–4)] starting from the *Herschel* LF by Gruppioni et al. and using appropriate $L_{\rm CO}$–$L_{\rm IR}$ conversions for different galaxy classes. Our predicted LFs fit the data so far available at $z \approx 0$ and 2. We compare our results with those obtained by semi-analytical models (SAMs): while we find a good agreement over the whole range of luminosities at $z \approx 0$, at $z \approx 1$ and $z \approx 2$, the tension between our LFs and SAMs in the faint and bright ends increases. We finally discuss the contribution of luminous active galactic nucleus ($L_X > 10^{44}$ erg s^{-1}) to the bright end of the CO LF concluding that they are too rare to reproduce the actual CO LF at $z \approx 2$.

Key words: galaxies: evolution – galaxies: luminosity function, mass function – infrared: galaxies.

1 INTRODUCTION

The study of the star formation (SF) history, and its connection with the gas mass accretion/consumption in galaxies, is one of the still open issues in modern cosmology. A proper description of the evolution of SF across cosmic time needs both (a) a thorough understanding of the relation between the total/molecular gas mass and the SF, and (b) sufficiently large samples of galaxies at different redshifts (z). As dust and gas are intimately associated, the dust infrared (IR) continuum emission can be a good proxy to infer the interstellar medium (ISM) mass (Scoville et al. 2014; Groves et al. 2015), tracing it on large samples across cosmic time (e.g. Berta et al. 2013). The state-of-the-art Atacama Large (Sub)Millimeter Array (ALMA) will make it possible in the next future to directly follow the molecular gas abundance as a function of redshift with blind searches of carbon monoxide (CO) rotational transitions (e.g. Carilli & Walter 2013, and references therein). So far, only a handful of observational works have attempted to constrain this quantity. Keres, Yun & Young (2003) measured for the first time the CO(1–0) luminosity function (LF) at $z = 0$ using far-infrared (FIR) and optical B-band selected samples (see also Boselli, Cortese & Boquien 2014, for more recent CO(1–0) data at $z \approx 0$). At $z \approx 2$, we have some observational constraints by Aravena et al. (2012) and Daddi et al. (2010). More recently, Walter et al. (2014) measured the CO LF in three redshift bins ($z \approx 0.3$, 1.52, 2.75) based on a blind molecular line scan using the IRAM Plateau de Bure Interferometer. In the near future, the advent of similar searches with ALMA will enable similar studies to much deeper levels and over larger areas. On the theoretical side, the method generally adopted to predict CO (J–(J–1)) LFs is to couple cosmological simulations with semi-analytical prescriptions that relate the CO emission to the physical properties of the simulated galaxies such as the intensity of the radiation field, the metallicity, the presence of an active galactic nucleus (AGN) (e.g. Obreschkow et al. 2009; Fu et al. 2012; Lagos et al. 2012; Popping, Somerville & Trager 2014a). The aim of this Letter is to derive the CO(1–0), CO(3–2), and CO(5–4) LFs at different redshifts by adopting a simple empirical approach that allows us to convert the state-of-the-art observed IR LF presented in Gruppioni et al. (2013). As a matter of fact, the CO luminosity is found to correlate with the total IR luminosity ($L_{\rm IR}$; 8–1000 μm), providing an integrated proxy of the Kennicutt–Schmidt (Kennicutt et al. 1998) relation that links star formation rate (SFR) and the molecular gas surface density. The correlation between these quantities relies on the fact that $L'_{\rm CO}$[1] is a molecular hydrogen tracer, while $L_{\rm IR}$ is a proxy of the SFR. This is true in homogeneous samples of galaxies with comparable ISM properties, as the correlation between $L_{\rm CO}$ and $L_{\rm IR}$ implicitly depends on the dust-to-gas ratios and metallicity within the galaxies (e.g. Leroy et al. 2013), on the presence of additional heating due to AGN activity which affects the temperature of dust grains, and on the effects of gas streaming motions on the star-forming properties (e.g. Meidt et al. 2013).

★ E-mail: livia.vallini@unibo.it

[1] In what follows the $L'_{\rm CO}$ notation will be used when the CO luminosity is expressed in K km s^{-1} pc^2.

2 METHOD

We derive the CO LF starting from the IR LF (Gruppioni et al. 2013) and converting it into CO LF through empirical $L'_{\rm CO}-L_{\rm IR}$ relations from the literature. To this purpose, we consider the Gruppioni et al. (2013) total IR LF based on deep and extended FIR (70−500 μm) data from the cosmological guaranteed time *Herschel* surveys, PACS Evolutionary Probe, (PEP; Lutz et al. 2011) and *Herschel* Multi-tiered Extragalactic Survey, (HerMES; Oliver et al. 2012), in the GOODS (GOODS-S and GOODS-N), Extended Chandra Deep Field South (ECDFS), and Cosmic Evolution Survey (COSMOS) areas. In Gruppioni et al. (2013), the authors have completely characterized the multiwavelength Spectral Energy Distributions (SEDs) of the PEP sources by performing a detailed SED-fitting analysis and comparison with known template libraries of IR populations. The sources have been classified on the basis on their broad-band SEDs in five main classes: spiral, reproduced by templates of normal spiral galaxies, starburst (SB) reproduced by templates of SB galaxies, AGN1, AGN2, reproduced by AGN-dominated SEDs (unobscured and obscured in the optical/UV), and SF-AGN reproduced by templates of Seyfert2/1.8/LINERS/Ultra Luminous Infrared Galaxies + AGN (i.e. the AGN emission might be present, although not dominant). The latter class is further divided into two sub-classes: AGN-SB and AGN-GAL on the basis of the far-IR/near-IR colours and on the evolutionary path. More precisely: the AGN-SB objects show an enhanced FIR flux typical of SB galaxies and dominate at high redshifts as the AGN-dominated sources, while AGN-GAL are characterized by an SED typical of normal spiral galaxies but with a low-luminosity AGN showing up in the mid-IR. For the shape of the LF, Gruppioni et al. (2013) assumed a modified Schechter function (Saunders et al. 1990), which depends on four parameters (α, σ, $L^{\star}_{\rm IR}$, and $\Phi^{\star}$). The parameters α and σ have been estimated at the redshift where the corresponding LF of each population is best sampled. This redshift is $z\approx 0$, except for the AGN1 and AGN2 classes which are more numerous and whose LF is better defined at $z\approx 2$. Subsequently, α and σ have been frozen leaving only $L^{\star}$ and $\Phi^{\star}$ free to vary. If we assume that the CO LF of each homogeneous class of objects has the same z-evolution of the corresponding IR LF, we can calculate the evolution of the total CO LF by adopting physically motivated conversions between IR and CO luminosities according to the properties of the galaxies composing each class. More precisely, $L_{\rm CO}$ and $L_{\rm IR}$ are generally found to be linked by a correlation of the form $\log(L'_{\rm CO}/{\rm K\,km\,s^{-1}\,pc^2}) = \alpha + \beta\log({\rm L_{IR}/L_{\odot}})$.

In the literature, there are many studies regarding the CO–IR relation in different samples of galaxies ranging from SB galaxies (e.g. Greve et al. 2014) to normal (main sequence, MS) ones (e.g. Sargent et al. 2014; Daddi et al. 2015). According to the definition of Rodighiero et al. (2011), the SB galaxies are the objects that, at each redshift, are more than ≈0.6 dex above the MS defined in the SFR–stellar mass plane. In the sample of Gruppioni et al. (2013), only AGN1, AGN2, and AGN-SB meet this criterium at all redshifts (cf. fig. 15 of Gruppioni et al. 2013); hence for these classes we will adopt the CO–IR relation found for SBs by Greve et al. (2014). In particular, Greve et al. (2014) provide for the first time IR/FIR–CO luminosity relations that extend up to $J_{\rm up}$= 13 based on *Herschel* SPIRE-FTS and ground-based telescopes data for local (U)LIRGs and high-z sub-millimeter galaxies. According to the notation introduced above, they found $\alpha\equiv\alpha_{\rm SB}=[-2.0, -2.2, -2.9]$ and $\beta\equiv\beta_{\rm SB}=[1.00, 1.00, 1.03]$ for the CO(1–0), CO(3–2), and CO(5–4) transitions, respectively.

On the other hand, in Gruppioni et al. (2013) galaxies with SEDs dominated by SF (spiral, SB, and AGN-GAL), especially at $z>1.2$, are below the threshold defined by Rodighiero et al. (2011) for SB galaxies. Thus, for these classes we will adopt the CO–IR conversion found by Sargent et al. (2014) for MS galaxies. More precisely, Sargent et al. (2014), considering a sample of $z\leq 3$ MS galaxies with CO detections, found that the CO(1–0) luminosity correlates with the IR with parameters $\alpha\equiv\alpha_{\rm MS}=0.54\pm0.02$ and $\beta\equiv\beta_{\rm MS}=0.81\pm0.03$. The 1σ scatter around the best-fitting relation is $\sigma_{\rm MS}=0.21$ dex. For higher-J transitions, we adopt the recent findings of Daddi et al. (2015) in which it has been shown that the relation between $L_{\rm IR}$ and the CO(5–4) luminosity is well described by a linear relation with $\alpha^{54}_{\rm MS}=-2.52$ and $\beta^{54}_{\rm MS}=1$. The dispersion in the residuals is 0.24 dex. To convert the $L'_{\rm CO}$(5–4) into the $L'_{\rm CO}$(3–2), we combine the average CO(3–2)/CO(1–0) flux ratio ($R_{31}=0.42\pm0.07$) and the CO(5–4)/CO(1–0) flux ratio ($R_{51}=0.23\pm0.04$) measured by the same authors within the same sample of galaxies. Although assuming conversion factors between different CO $(J-(J-1))$ transitions represents a strong assumption, our choice is motivated by the lack of explicit studies regarding the CO(3–2)–IR relation in MS galaxies. Ultimately, to obtain the total CO LF at various redshifts, we combine the LF of each class after having conveniently re-binned each of them within equal CO luminosity bins.

3 RESULTS

In Fig. 1, we show with solid lines the CO(1–0), CO(3–2), and CO(5–4) LFs at $z\approx 0, 1, 2$ as obtained through the method described in the previous section. The LFs are colour-coded as a function of the transition, with shaded regions representing the uncertainties on the prediction due to the scatter in the CO–IR relation. More precisely, the upper limit is obtained by adopting the conversion factors from Sargent et al. (2014) and Daddi et al. (2015) for all the populations and considering the maximum in their $L'_{\rm CO}-L_{\rm FIR}$ relation; the lower bound is obtained by considering the minimum in the $L'_{\rm CO}-L_{\rm FIR}$ relation from Greve et al. (2014). We find that our fiducial model is consistent with the observed points at $z=0$ (Keres et al. 2003) and the upper limit by Walter et al. (2014). The same holds true for the CO(1–0) LF at $z\approx 1$, even though it must be noticed that data point by Walter et al. (2014) refers to a slightly higher redshift ($z\approx 1.5$). The lower (upper) limits of the Walter et al. (2014) data are obtained considering only secure detections (all candidates). At $z\approx 2$, the CO(1–0) observations by Aravena et al. (2012) and Daddi et al. (2015), and the CO(3–2) data point at $z\approx 2.7$ by Walter et al. (2014) are well consistent with our LFs. However, it must be noticed that, on average, the estimate by Walter et al. (2014) of the number densities is systematically higher with respect to our predictions. We also compare our results with predictions of semi-analytical models (SAMs) by Obreschkow et al. (2009); Fu et al. (2012); Lagos et al. (2012), and with the CO LFs obtained by Popping et al. (in preparation) based on the model presented in Popping et al. (2014a), where the authors coupled the Popping et al. (2014b) SAMs with a radiative transfer code. While our results and SAMs are fairly in agreement over the whole range of luminosities at $z\approx 0$, at $z\approx 1$, and $z\approx 2$, they increasingly disagree at the faint and bright ends. The difference in the faint end can be explained by considering two concurrent reasons. The first one is the well-known excess of low/intermediate-mass galaxies predicted by most SAMs with respect to the observed mass functions. The second one is related to the fact that the slope of the faint-end of the

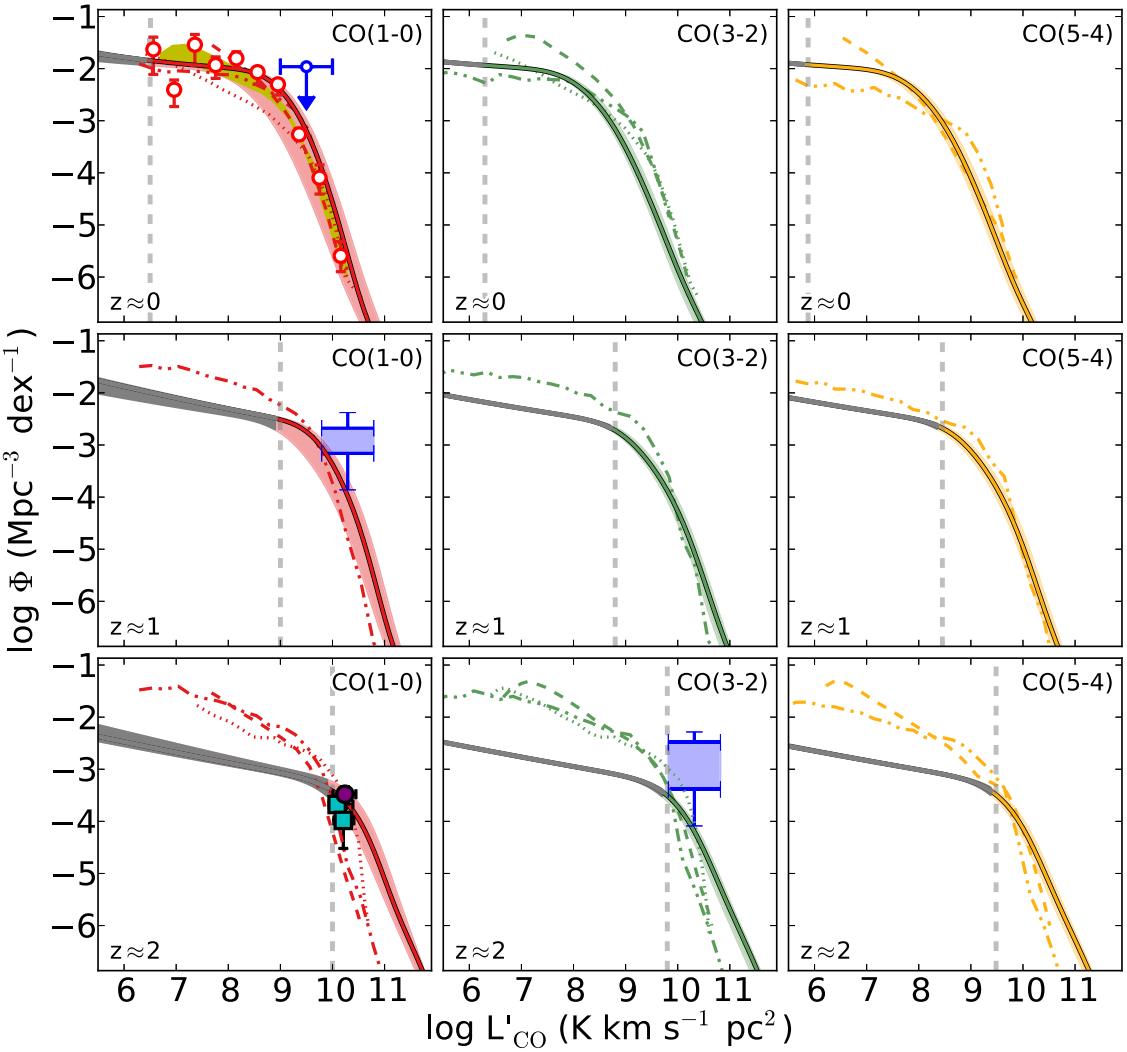

Figure 1. From left to right: CO(1–0), CO(3–2), and CO(5–4) luminosity functions (LFs), at $z \approx 0$ (upper row), $z \approx 1$ (middle row), and $z \approx 2$ (bottom row). Coloured solid lines with shaded regions represent our prediction with the corresponding uncertainty. The faint-end extrapolation of the CO LFs is plotted in grey and the luminosity limit of the underlying IR LFs is highlighted with a vertical dashed line. Open circles at $z \approx 0$ are the data from Keres et al. (2003), while cyan squares at $z \approx 2$ are the space densities derived from CO detections presented in Aravena et al. (2012) and corrected for the overdensity of the field in which the observation was performed. The purple circle in the same panel represents the data by Daddi et al. (2010) from the BzK star-forming galaxies. The recent CO(1–0) and CO(3–2) data from Walter et al. (2014) with their error bars are plotted in blue. Dashed, dotted, and dash–dotted lines are instead the predictions from semi-analytical models by Obreschkow et al. (2009); Lagos et al. (2012) and Popping et al. (in preparation), respectively. The yellow shaded region in the first panel highlights the parameter space covered by the three different models for the CO(1–0) LF at $z \approx 0$ discussed by Fu et al. (2012).

observed IR LFs is derived at $z \approx 0$, where the LF is better covered by the data and kept fixed in all the redshift bins. This means that at $z \approx 2$, where the faint end is not covered by the IR data (light grey regions in Fig. 1), the slope is not constrained by the observations. We note that, above this limit, our CO(1–0) LF at $z \approx 2$ reproduces the observed data from Aravena et al. (2012). The overprediction of the bright-end at $z \approx 2$ with respect to the SAMs shows up especially for the CO(1–0) transition that is the one more closely related to the SF and scarcely affected by the AGN activity. Not surprisingly, the same trend has been recently found by Gruppioni et al. (2015) when comparing the SFR function derived from IR luminosity (due to the SF only) with the SFR function predicted by four different SAMs. These discrepancies might be connected either to wrong photometric redshifts and source confusion that might enhance the bright-end of the *Herschel* IR LF, or to the difficulty of SAMs in modelling the AGN feedback that affects the inflow/outflow of gas in the largest and most massive galaxies. We note that for high-J CO transitions the tension between our LFs and SAMs at $z \approx 2$ is less obvious. However, high-J CO lines luminosities are strongly dependent on the CO Spectral Line Energy Distribution that varies from galaxy to galaxy. We have tested that if, instead of adopting the $L'_{CO}(J-(J-1))$–*IR* relation provided by Greve et al. (2014) to convert the IR LF of SB galaxies, we consider the maximum and minimum $L'_{CO}(3-2)/L'_{CO}(1-0)$ ($L'_{CO}(5-4)/L'_{CO}(1-0)$) ratios within the same sample and we convert the CO(1–0) LF into the corresponding CO(3–2) and CO(5–4) the variation of the bright-end can be > 1 dex.

We now exploit the potential of the LF decomposition by Gruppioni et al. (2013) to separFately analyse the relative contribution to the total CO LF of galaxies populations with a significant AGN activity (i.e. AGN1, AGN2, and AGN-SB). The contribution of these classes is shown with red dashed lines in Fig. 2.

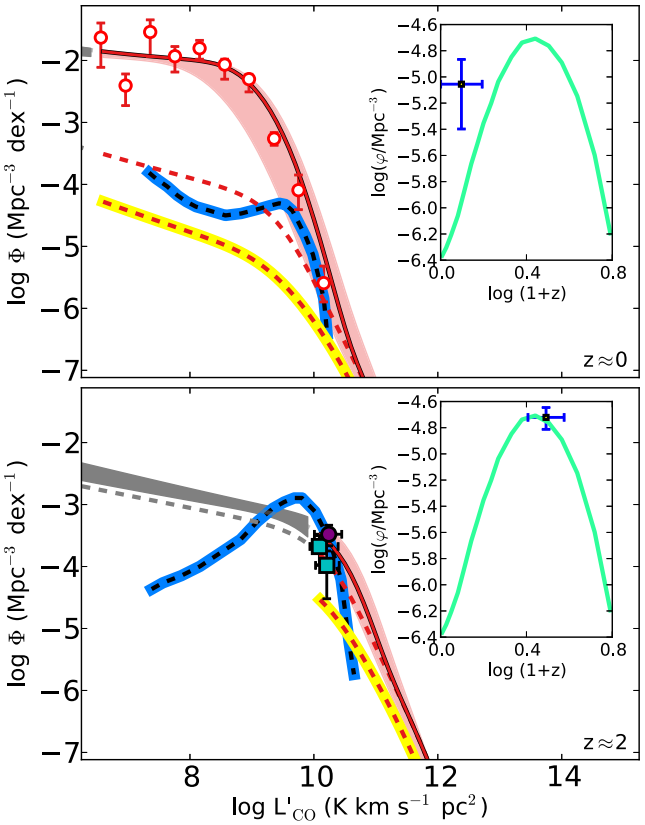

Figure 2. CO(1–0) LF at $z \approx 0$, 2 as predicted by our model. The blue dashed lines indicate the contribution AGN-dominated galaxies (L_X(2–10 keV) $> 10^{44}$ erg s^{-1}) by Lagos et al. (2012), while the red dashed lines represent our results for the sum of AGN1, AGN2, and AGN-SB. The resulting LF, up to the luminosity limit, corrected for the fraction of AGN with $L_X > 10^{44}$ erg s^{-1}, is highlighted in yellow. In the upper/lower inset, we plot in blue the number density (φ) resulting from the integration of the corrected AGN1, AGN2, and AGN-SB LFs up to their luminosity limit at $z \approx 0$ and $z \approx 2$, respectively. The cyan solid line represents φ for AGN with $44 < \log(L_x/\mathrm{erg\,s^{-1}}) < 45$ by Aird et al. (2015).

In the same figure, blue dashed lines indicate the theoretical prediction by Lagos et al. (2012) for galaxies that host bright AGN (L_X(2–10 keV) $> 10^{44}$ erg s^{-1}). Lagos et al. (2012) found that bright AGN are responsible for most of the evolution with z of the bright-end of the CO LF. However, the classification proposed by Lagos et al. (2012) is not directly comparable to the one adopted in Gruppioni et al. (2013) to identify AGN-dominated galaxies. As a matter of fact, in Gruppioni et al. (2013), the selection is based on the typical SED of the objects composing the class regardless of the intrinsic L_X of these galaxies. Thus, to make a more meaningful comparison, we estimate the fraction of AGN1, AGN2, and AGN-SB with $L_X > 10^{44}$ erg s^{-1}. To this purpose, for the sources detected in X-rays, we use the measured L_X, while for the undetected ones, we convert the total intrinsic luminosity of the accretion disc of AGN (bolometric luminosity; $L_{\rm bol}$) into the corresponding X-ray (2–10 keV) luminosity through the X-ray bolometric correction $L_X = L_{\rm bol}/k_{\rm bol}(L_{\rm bol})$ as in Marconi et al. (2004). The $L_{\rm bol}$ has been computed by Delvecchio et al. (2014) through an SED decomposition analysis performed on the same sample considered in Gruppioni et al. (2013). In Fig. 3, we plot the X-ray luminosity, as obtained by the procedure described above, as a function of the $L'_{\rm CO}$ for AGN1, AGN2, and AGN-SB. We note that the points align along two parallel sequences: the higher one is populated mainly by sources that,

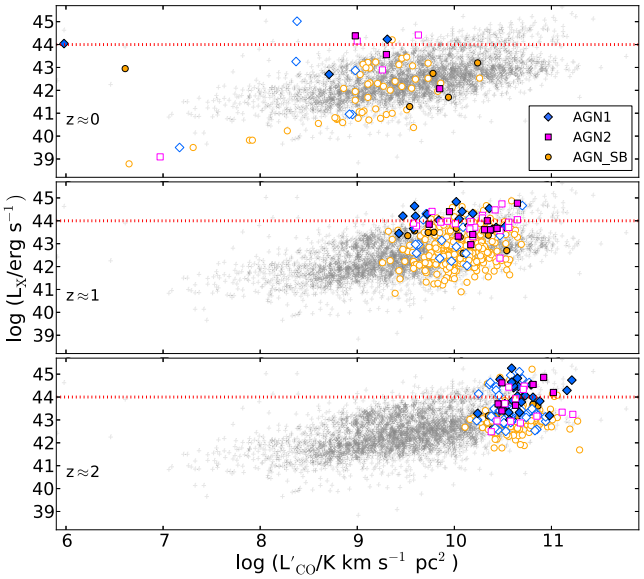

Figure 3. L_X as a function of the CO(1–0) luminosity for AGN1 (blue diamonds) AGN2 (magenta squares) and AGN_SB (orange circles) at $z \approx 0$, 1, 2 (upper/middle/lower panel). Filled symbols represent objects for which the X-ray luminosities are measured, while open symbols are used for sources that are non-detected in X-ray whose L_X is computed through the $L_{\rm bol}$. For reference, the whole sample at all redshifts, including the spirals, SB, AGN-GAL is plotted with grey crosses. We highlight with a red dotted line the limit $L_X = 10^{44}$ erg s^{-1}.

according to the SED decomposition by Gruppioni et al. (2013), are AGN dominated (AGN1, AGN2), while the lower one is characterized by galaxy-dominated objects (AGN-SB). Moreover, even though $L_{\rm bol}$ and L'_{CO} are not completely independent, being both indirectly based on the SED fit, no strong correlation is found between these two quantities within the same redshift range. This implies that the correction factor that we must apply to our LF in order to match with the Lagos et al. (2012) criterium can be assumed to be constant over the interval over which we have data. However, it is impossible to apply any correction to the faint end extrapolation of the CO LF because in that range we have no clues on the actual value of the $L_{\rm bol}$ (and thus of the L_X) with respect to the IR luminosity.

The correction factor (f_X) is calculated by considering the cumulative distribution function of the L_X within the AGN1, AGN2, and AGN-SB classes. We find that at $z \approx 0$ the fractions of AGN1, AGN2, and AGN-SB with $L_X > 10^{44}$ erg s^{-1} are, respectively, $f_X = [0.3, 0.4, 0.02]$, while at $z \approx 2$ they are $f_X = [0.4, 0.3, 0.09]$. The resulting CO LFs after correcting by the f_X the bins in which we have data, are highlighted in yellow in Fig. 2. We note that, once we correct our sample for the L_X threshold, our predictions are substantially lower than the theoretical one by Lagos et al. (2012). In principle, a possible way to explain this discrepancy would be that some of the sources identified by Gruppioni et al. (2013) as dominated by SF (spiral, SB, AGN-GAL) could instead host AGN as powerful as $L_X > 10^{44}$ erg s^{-1}. However, we verified that $f_X = 0$ for the objects in these classes. To further test the consistency of our predictions, we calculate the number density of AGN with $L_X > 10^{44}$ erg s^{-1} by integrating up to the luminosity limit the corrected AGN1, AGN2, AGN-SB LFs, and we compare the result with the number density (φ) of objects with $44 < \log(L_x/\mathrm{erg\,s^{-1}}) < 45$ found by Aird et al. (2015) using X-ray surveys, achieving a good consistence at $z \approx 2$ but a higher value,

although with a large uncertainty, at $z \approx 0$ (see Fig. 2). This implies that our predicted LF, although significantly lower than that of Lagos et al. (2012), yields a number density larger with respect to the number density of AGN with $L_X > 10^{44}$ erg s^{-1} derived from X-ray data. Note that the higher value of φ found at $z \approx 0$ from our IR-based work might be due to an underestimate either of the Compton thick fraction or of the obscuration correction for some X-ray sources (i.e. classified as $L_X < 10^{44}$ erg s^{-1} although intrinsically brighter). After having excluded the hypothesis of missing a substantial fraction of objects with $L_X > 10^{44}$ erg s^{-1} because accounted in other classes, we derived the 3σ upper limits on the rest frame 2–10 keV luminosities for the objects in the Aravena et al. (2012) sample using the *XMM–Newton* data. To this purpose, we adopted the 0.5–2 keV sensitivity map, which takes into account the effects of vignetting; the choice of this band is motivated by the high throughput of *XMM–Newton* at soft X-ray energies. Assuming a power-law model with photon index $\Gamma = 1.7$, we obtain that all the sources have $L_X < 3.5 \times 10^{43}$ erg s^{-1}. This results is in agreement with our prediction that the data points by Aravena et al. (2012) should not contain $L_X > 10^{44}$ erg s^{-1} AGN and therefore further support our hypothesis that the bright end of the CO LF, while mainly produced by sources that are likely AGN hosts, do not show up as extremely luminous.

4 DISCUSSION AND CONCLUSIONS

We calculated the CO(1–0), CO(3–2), and CO(5–4) LFs at $z \approx 0$, 1 and 2 by starting from the redshift evolution of the state-of-the-art IR LF presented in Gruppioni et al. (2013). We obtain the CO LF by coupling the IR LF with $L_{\rm IR}-L'_{\rm CO}$ conversions specifically tailored for each class of galaxies that compose the IR LF. Our empirical approach reproduces well the observed data/upper limits at $z \approx 0$ and $z \approx 2$. This is an encouraging validation of our assumption that the redshift evolution of the CO and IR LF are closely related. As a caveat, we must note that, especially at $z \approx 2$, there are tensions between the predictions of the faint (and bright) end as resulting from our approach, and those obtained by SAMs. These discrepancies might be explained by several concurring reasons either on the theoretical side (e.g. difficulties in modelling feedbacks) and/or on the observational side (e.g. uncertainties in the photometric redshifts). Moreover we cannot rule out the possibility that towards $z \approx 2$ and above, the evolution of IR and COs LFs might be different. Finally we demonstrate that, although AGN-dominated galaxies account for the bright end of the CO LF, at $z \approx 2$ we are able to reproduce the observed points above the knee of the CO LF only if we include all the AGN-dominated galaxies in our sample, regardless of their X-ray (2–10 keV) luminosity. More precisely, AGN with $L_X > 10^{44}$ erg s^{-1} that have been predicted by previous studies to completely account for the bright end of the CO LF are too rare to reproduce the actual CO LF at $z \approx 2$.

ACKNOWLEDGEMENTS

We are grateful to G. Popping for having provided the CO LFs as resulting from his work in preparation. We thank the anonymous referee for her/his insightful comments that improved significantly the Letter.

REFERENCES

Aird J., Coil A. L., Georgakakis A., Nandra K., Barro G., Pérez-González P. G., 2015, MNRAS, 451, 1892
Aravena M. et al., 2012, MNRAS, 426, 258
Berta S. et al., 2013, A&A, 555, L8
Boselli A., Cortese L., Boquien M., 2014, A&A, 564, A65
Carilli C., Walter A., 2013, ARA&A, 51, 105
Daddi E. et al., 2010, ApJ, 713, 686
Daddi E. et al., 2015, A&A, 577, A46
Delvecchio I. et al., 2014, MNRAS, 439, 2736
Fu J., Kauffmann G., Li C., Guo Q., 2012, MNRAS, 424, 2701
Greve T. R. et al., 2014, ApJ, 794, 142
Groves B. A. et al., 2015, ApJ, 799, 96
Gruppioni C. et al., 2013, MNRAS, 432, 23
Gruppioni C. et al., 2015, MNRAS, 451, 3419
Kennicutt R. C. Jr, et al., 1998, ApJ, 498, 181
Keres D., Yun M. S., Young J. S., 2003, ApJ, 582, 659
Lagos C. d. P., Bayet E., Baugh C. M., Lacey C. G., Bell T. A., Fanidakis N., Geach J. E., 2012, MNRAS, 426, 2142
Leroy A. K. et al., 2013, AJ, 146, 19
Lutz D. et al., 2011, A&A, 532, A90
Marconi A., Risaliti G., Gilli R., Hunt L. K., Maiolino R., Salvati M., 2004, MNRAS, 351, 169
Meidt S. E. et al., 2013, ApJ, 779, 45
Obreschkow D., Heywood I., Klöckner H.-R., Rawlings S., 2009, ApJ, 702, 1321
Oliver S. J. et al., 2012, MNRAS, 424, 1614
Popping G., Somerville R. S., Trager S. C., 2014a, MNRAS, 442, 2398
Popping G., Pérez-Beaupuits J. P., Spaans M., Trager S. C., Somerville R. S., 2014b, MNRAS, 444, 1301
Rodighiero G. et al., 2011, ApJ, 739, L40
Sargent M. T. et al., 2014, ApJ, 793, 19
Saunders W., Rowan-Robinson M., Lawrence A., Efstathiou G., Kaiser N., Ellis R. S., Frenk C. S., 1990, MNRAS, 242, 318
Scoville N. et al., 2014, ApJ, 783, 84
Walter F. et al., 2014, ApJ, 782, 79

This paper has been typeset from a TEX/LATEX file prepared by the author.